

SPECTROSCOPY OF ^{54}Mn

BY J. GASTEBOIS, J. KUŹMIŃSKI* AND J. M. LAGET

Service de Physique Nucléaire à Basse Energie, Centre d'Etudes Nucléaires de Saclay, France

(Received October 17, 1970)

The experimental results of the $^{52}\text{Cr}(^3\text{He}, p)^{54}\text{Mn}$, $^{53}\text{Cr}(^3\text{He}, d)^{54}\text{Mn}$ reactions, performed at $E(^3\text{He}) = 18$ MeV, and the results of the $^{56}\text{Fe}(d, \alpha)^{54}\text{Mn}$ reaction, performed at $E(d) = 12$ MeV, are presented. The experimental data are analyzed in the frame work of the D. W. B. A. theory. The main conclusion of this study is that the configuration mixing is important, even in the ^{54}Mn low lying state wave functions.

1. Introduction

The spectroscopy of ^{54}Mn was not yet extensively studied. The excitation energies of the ^{54}Mn low lying levels was deduced by Bjerregaard *et al.* [1] from the study of the $^{56}\text{Fe}(d, \alpha)^{54}\text{Mn}$ reaction at $E(d) = 4$ MeV. Zeidmann *et al.* [2] have studied the $^{55}\text{Mn}(d, t)^{54}\text{Mn}$ reaction at $E(d) = 21.6$ MeV, and Legg *et al.* [3] have performed the $^{55}\text{Mn}(p, d)^{54}\text{Mn}$ reaction at $E(p) = 22$ MeV. They deduce the value of the orbital momentum of the picked neutron [2, 3] and they extract the spectroscopic factor [3] for the most intense transitions to some low lying levels of ^{54}Mn . The ^{54}Mn low lying level scheme was also studied through the $^{53}\text{Cr}(p, \gamma)^{54}\text{Mn}$ reaction [4]. On the other hand Vervier [5] has computed the wave function of ^{54}Mn low lying states, assuming that the active nucleons belong to the $[(\pi f_{7/2})^5, \nu p_{3/2}]_J \pi$, $[(\pi f_{7/2})^5, \nu f_{5/2}]_J \pi$, $[(\pi f_{7/2})^5, \nu p_{1/2}]_J \pi$ configurations.

In this paper we present the result of the study of the $^{52}\text{Cr}(^3\text{He}, p)^{54}\text{Mn}$, $^{53}\text{Cr}(^3\text{He}, d)^{54}\text{Mn}$ reactions performed at $E(^3\text{He}) = 18$ MeV, and the results of the $^{56}\text{Fe}(d, \alpha)^{54}\text{Mn}$ reaction study performed at $E(d) = 12$ MeV.

2. Experimental procedure and results

We have used the 18 MeV ^3He beam and the 12 MeV deuteron beam of the Saclay Tandem Van de Graaff. The targets were obtained by vacuum evaporation of ^{52}Cr (99.9%), ^{53}Cr (96.4%) and ^{56}Fe (99.9%) enriched isotopes. The ^{52}Cr and ^{53}Cr targets were carbon

* Address: Instytut Fizyki, Uniwersytet Śląski, Katowice, Bankowa 12, Poland

backed ($15 \mu\text{g}/\text{cm}^2$) and were respectively $50 \mu\text{g}/\text{cm}^2$ and $70 \mu\text{g}/\text{cm}^2$ thick. The self supporting ^{56}Fe one was $115 \mu\text{g}/\text{cm}^2$ thick.

The experimental set up has been previously described [6].

2.1. The $^{52}\text{Cr}(^3\text{He}, p)^{54}\text{Mn}$ reaction

The proton spectrum obtained at $\theta_{\text{Lab}} = 32^\circ$ is shown in Fig. 1. The overall energy resolution is about 60 keV (F. W. H. M.). The energy calibration has been deduced from the energies of protons due to target impurities (namely ^{12}C and ^{16}O). The energies of the excited groups are listed in Table I and they are in good agreement with the previously known values [1]. Due to our energy resolution many of these groups may be unresolved multiplets. The cross-sections of the $(^3\text{He}, p)$ transitions to the first three excited states are

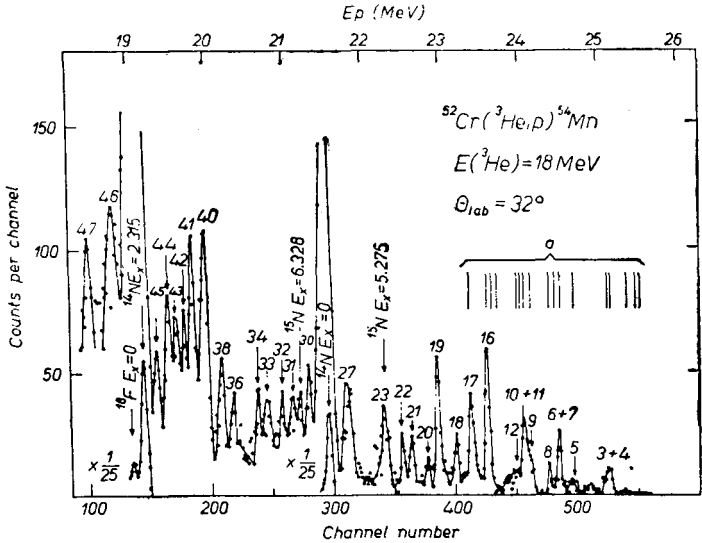


Fig. 1. Proton spectrum from the $^{52}\text{Cr}(^3\text{He}, p)^{54}\text{Mn}$ reaction. Previously known levels [1] are labelled "a".

very low: the corresponding proton groups are only seen at a few angles. The absolute cross-section values have been obtained by comparison between proton yields and the $^{52}\text{Cr}(^3\text{He}, ^3\text{He})^{52}\text{Cr}$ elastic scattering yield at $\theta_{\text{Lab}} = 20^\circ$ and $E(^3\text{He}) = 15 \text{ MeV}$. They are believed to be systematically in error by about 20%. We have listed in Table I the values of the absolute cross-sections integrated between $\theta = 10^\circ$ and $\theta = 80^\circ$, and the value of the absolute cross-section at $\theta_{\text{Lab}} = 32^\circ$. The statistical errors only are given.

The proton angular distributions corresponding to 19 groups have been obtained from $\theta_{\text{Lab}} = 10^\circ$ to $\theta_{\text{Lab}} = 80^\circ$. They are shown in Fig. 2a and Fig. 2b. The curves have been computed, in the D. W. B. A. framework, following the Glendenning's formalism [7], as described in Ref. [6]. The optical potential parameters we have used are listed in Table II. The L values obtained in this analysis are given in Table I. Most of the transitions are governed by an $L = 2$ transferred angular momentum. Only the transitions to the 0.387 MeV groups (Nb 3+4) and to the 6.127 MeV level (Nb 45) are respectively characterized by

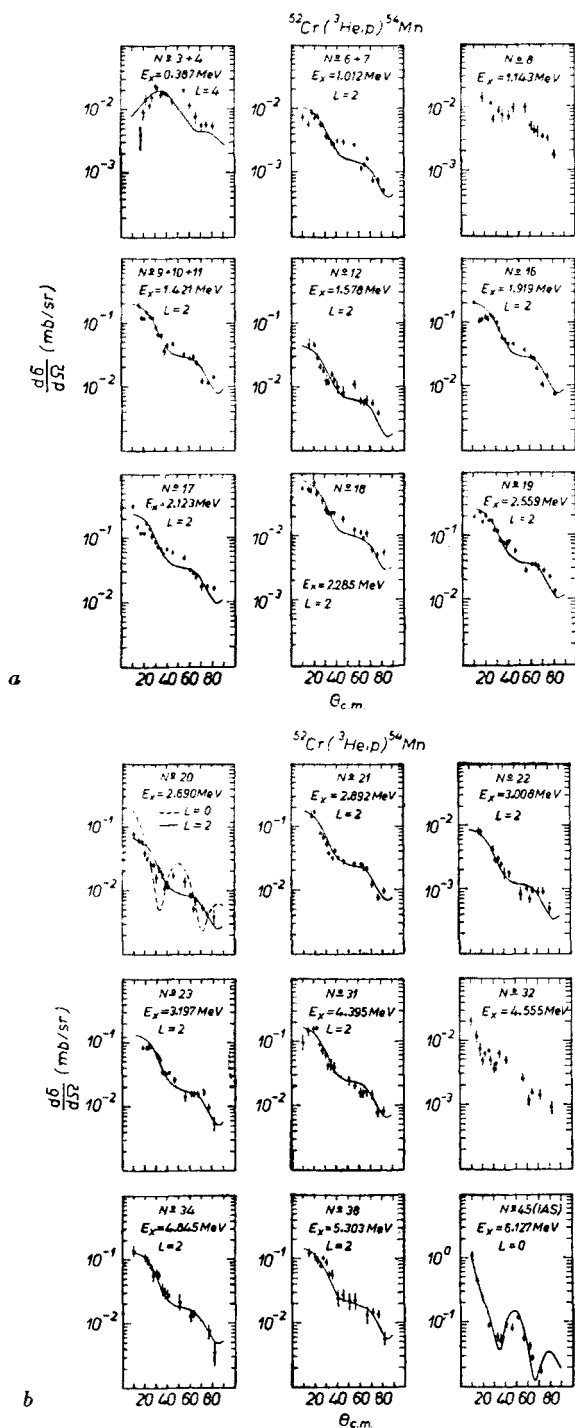


Fig. 2a. Angular distributions of protons from the $^{52}\text{Cr}(^3\text{He},p)$ reaction. Solid lines are D.W.B.A. curves
 Fig. 2b. See caption of Fig. 2a

TABLE I

Experimental results of the $^{52}\text{Cr}(^3\text{He}, p)^{54}\text{Mn}$ reaction

Group Nb	$E_x(\text{keV})$ a)	J^π b)	$E_x(\text{keV})$ c)	L c)	$\frac{\partial\sigma}{\partial\Omega} \Big _{32.0^\circ}$ $\mu\text{b}/\text{sr c}$	$2\pi \int_{10^\circ}^{80^\circ} \frac{\partial\sigma}{\partial\Omega} \sin\theta \, d\theta$ $\mu\text{b c}$
0	0	3 ⁺	d)			
1	56±12		d)			
2	156±12		d)			
3	365±12		387±30	4	22.4±2.6	63±7
4	405±12					
5	837±12		814±30		10.4±2.1	
6	1008±12		1012±30	2	33.9±3.5	134±14
7	1074±12					
8	1137±12		1143±30	(0)	8.7±1.7	34±6
9	1376±12		1372±30			
10	1455±12		1421±30	2	65.5±5.0	218±17
11	1511±12					
12	(1543±12)		1574±30	2	12.2±2.1	53±9
13			d)			
14	1784 ±12		d)			
15	1859±12		d)			
16	1924±12		1919±30	2	79.0±7.0	237±21
17	2137±12		2123±30	2	73.0±5.0	289±20
18			2285±30	2	22.3±3.5	94±14
19			2559±30	2	85.4±7.0	318±50
20			2690±30	(0,2)?	22.1±4.0	74±12
21			2892±30	2	37.2±4.2	160±18
22			3008±30	2	29.0±4.2	94±13
23			3197±30	2	54.3±5.6	135±13
24			d)			
25			d)			
26			d)			
27			3693±30		103 ±9.0	
28			d)			
29			d)			
30			4197±30		91.2±8.4	
31			4395±30		41.9±5.7	
32			4555±30	(0)	43.4±7.7	176±31
33			4719±30		35.4±7.0	
34			4845±30		56.5±9.1	
35			d)			
36			5159±30		42.0±8.5	
37			d)			
38			5303±30		56.2±9.2	166±27
39			d)			
40			5520±30		20.0±1.3	487±30
41			5677±30		13.4±1.2	455±41
42			5773±30		81.5±9.2	

Table I (continued)

Group Nb	$E_x(\text{keV})$ a)	J^π b)	$E_x(\text{keV})$ c)	L c)	$\frac{\partial \sigma}{\partial \Omega} \Big _{32.0^\circ}$ ($\mu\text{b}/\text{sr}$ c)	$2\pi \int_{10^\circ}^{80^\circ} \frac{\partial \sigma}{\partial \Omega} \sin \theta d\theta$ $10^\circ \mu\text{b}$ c)
43			5877 ± 30	0	96.0 ± 10.0	409 ± 69
44			5971 ± 30		106.0 ± 11.0	
45			6127 ± 30		58.7 ± 10.0	
46			6680 ± 30		292.0 ± 19.0	
47			6983 ± 30		111.0 ± 14.0	

a) previously known values, b) see Ref. [14], c) this work, d) transition corresponding to this level seen in the $^{53}\text{Cr}(^3\text{He}, d)$ ^{54}Mn reaction.

TABLE II

Optical potentials used in the $^{52}\text{Cr}(^3\text{He}, p)$ ^{54}Mn reaction analysis a)

	V MeV	W MeV	r_0 fm	r_c fm	a fm	r'_0 fm	a' fm	W' MeV	V_{SO} MeV
^3He b)	165	20.2	1.14	1.3	0.723	1.6	0.81	0	0
p c)	50.8	0	1.25	1.25	0.65	1.25	0.47	9.18	7.5

a) The optical potential used has the form

$$V(r) = -V(1 + \exp x)^{-1} - i \left(W - 4W' \frac{d}{dx} \right) (1 + \exp x')^{-1} + \left[\frac{\hbar}{m_\pi c} \right]^2 V_{\text{SO}} \frac{1}{r} \frac{d}{dr} (1 + \exp x)^{-1} \vec{L} \cdot \vec{\sigma} + V_c(r_c, r)$$

where $x = (r - r_0 A^{1/3})/a$, $x' = (r - r'_0 A^{1/3})/a'$ and $V_c(r_c, r)$ is the Coulomb potential. b) Values given in Ref. [15]. c) Values deduced from reference [16].

a $L=4$ and $L=0$ transferred angular momentum. The shape of the proton angular distributions corresponding to the levels Nb 8, 20 and 32 at $E_x = 1.143$ MeV, $E_x = 2.690$ MeV and $E_x = 4.555$ MeV seems to show that the expression of the transition amplitude contains an $L=0$ component. However these levels are weakly excited, and the D. W. B. A. analysis of the associated angular distribution is inconclusive.

The analogue state, in ^{54}Mn , of the $J^\pi = 0^+$ ground state of ^{54}Cr is predicted at $E_x = 6.144 \pm 0.045$ MeV, as it can be deduced from the Coulomb displacement value $\Delta E_c = 8.305 \pm 0.040$ MeV for the $^{54}\text{Cr} - ^{54}\text{Mn}$ isobaric pair [8], and from the ground state Q value ($Q = -2.161 \pm 0.005$ MeV) of the $^{54}\text{Cr}(p, n)$ ^{54}Mn reaction [9]. The proton angular distribution, associated with the state number 45, has a characteristic $L=0$ pattern, and the excitation energy $E_x = 6.127 \pm 0.030$ MeV leads us to identify this state with the analogue state of the $^{54}\text{Cr}(J^\pi = 0^+)$ ground state.

2.2. The $^{53}\text{Cr}({}^3\text{He}, d){}^{54}\text{Mn}$ reaction

In Fig. 3 we give the experimental deuteron spectrum obtained at $\theta_{\text{Lab}} = 32^\circ 5$. The overall energy resolution is about 60 keV (F. W. H. M.). The energy calibration has been deduced from the known energies of the deuteron groups corresponding to the most in-

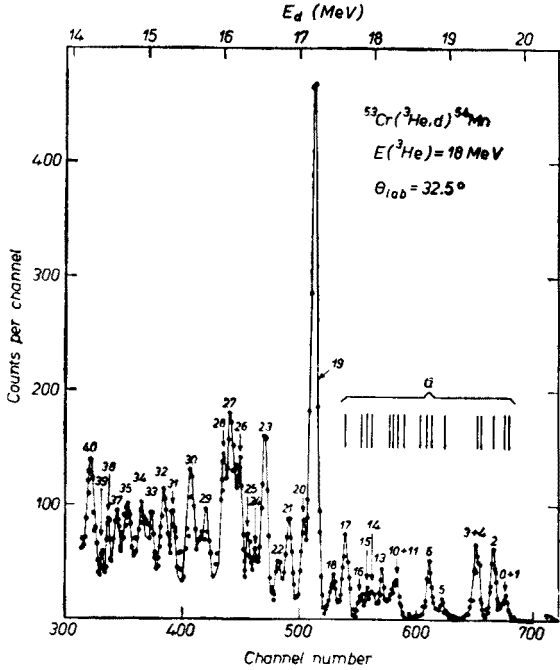


Fig. 3. Deuteron spectrum from the $^{53}\text{Cr}({}^3\text{He}, d){}^{54}\text{Mn}$ reaction. Previously known levels are labelled “a”.

tense transitions. The deduced excitation energies are listed in Table III (the level numbering is the same as in Table I). Due to our energy resolution many of these groups may be unresolved multiplets. The values of the absolute cross-sections have been obtained by comparison between the deuteron yields and the ${}^3\text{He}$ elastic scattering yield at $\theta_{\text{Lab}} = 20^\circ$ and $E({}^3\text{He}) = 15 \text{ MeV}$. They are believed to be systematically in error by about 20%. The values of the absolute cross-sections integrated between $\theta = 10^\circ$ and $\theta = 50^\circ$, and those of the absolute cross-sections at $\theta_{\text{Lab}} = 32^\circ 5$ are listed in Table II (only statistical errors are given).

The deuteron angular distributions have been obtained, from $\theta_{\text{Lab}} = 10^\circ$ to $\theta_{\text{Lab}} = 50^\circ$, for 24 transitions. They are shown in Figs 4a and 4b. The curves have been computed using the Julie code [10]. The parameters of the optical potentials and those used in the computation of the captured proton wave function, are given in Table IV. The orbital momentum values l of the transferred proton, deduced from the D. W. B. A. analysis of the angular distributions, are listed in Table III. We have also extracted spectroscopic factors from the comparison between the experimental integrated cross-section values, and those computed

TABLE III

Experimental results of the $^{53}\text{Cr}(^3\text{He}, d) ^{54}\text{Mn}$ reaction

Group Nb	E_x (keV) a)	J^π b)	E_x (keV) c)	L c)	$\frac{\partial\sigma}{\partial\Omega}\bigg _{32.5^\circ}$ $\mu\text{b/sr}$	$2\pi\int_{10}^{50}\frac{\partial\sigma}{\partial\Omega}\sin\theta d\theta$ $\mu\text{b c)}$	$\frac{2J_f+1}{2J_0+1}C^2S$	
0	0	3 ⁺	}	0	3	}	}	}
1	56±12			3	}			
2	156±12		3	}		}	}	
3	365±12		}		359±25			}
4	405±12			}		809±25	}	
5	837±12		}		1003±25			}
6	1008±12			}		d)	}	
7	1074±12		}		d)			}
8	1137±12			}		d)	}	
9	1376±12		}		d)			}
10	1455±12			}		1457±25	(1)	
11	1511±12		}		d)			}
12	(1543±12)			}		1636±25	1	
13			}		1785±25			(1)
14	1784±12			}		1913±25	}	
15	1859±12		}		2116±25			1
16	1924±12			}		2268±25	1	
17	2137±12		}		2559±25			1
18				}		2675±25	(1)	
19			}		2881±25			1
20				}		3013±25	1	
21			}		3213±25			1
22				}		3337±25	1	
23			}		3419±25			1
24				}		3549±25	1	
25			}		3670±25			1
26				}		3736±25	1	
27			}		4002±25			1
28				}		4197±25	1	
29			}		4421±25			1
30				}		4554±25	1	
31			}		4742±25			}
32				}		4851±25	}	
33			}		5029±25			}
34				}		d)	}	
35			}		5217±25			}
36				}		5320±25	}	
37			}		5429±25			}
38				}		5503±25	}	
39			}					}
40		}				}	}	

a) Previously known values [1]. b) See Ref. [14]. c) This work. d) Transition corresponding to this level seen in the $^{52}\text{Cr}(^3\text{He}, p) ^{54}\text{Mn}$ reaction.

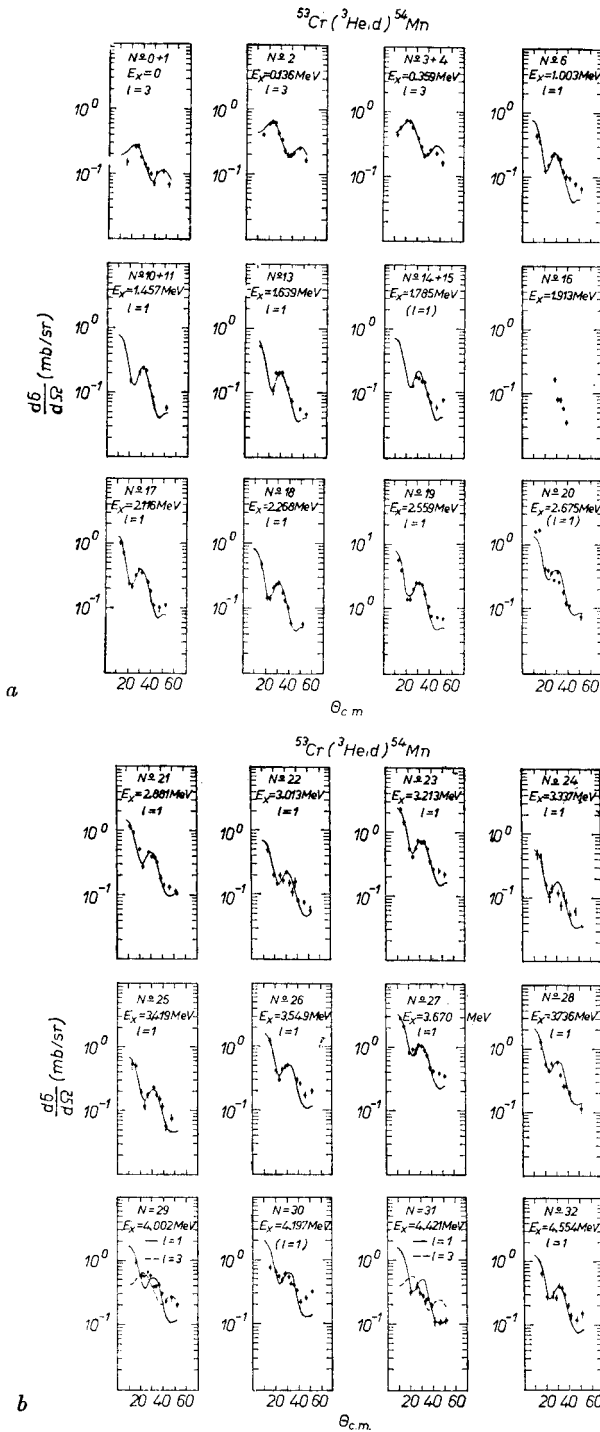


Fig. 4a. Angular distributions of deuterons from the $^{53}\text{Cr}(^3\text{He}, d)^{54}\text{Mn}$ reaction. Solid lines are D.W.B.A. curves
Fig. 4b. See caption of Fig. 4a

TABLE IV

Optical potentials used in the $^{53}\text{Cr}(^3\text{He}, d) ^{54}\text{Mn}$ reaction analysis ^{a)}

	V MeV	W MeV	r_0 fm	r_c fm	a fm	r'_0 fm	a' fm	W' MeV	V_{SO} MeV
^3He b)	165	20.2	1.14	1.3	0.723	1.6	0.81	0	0
d c)	93.3	0	1.15	1.15	0.810	1.34	0.68	16.9	0
p	d)	0	1.25	1.25	0.650	0	0	0	e)

^{a)} See footnotes of Table II. ^{b)} Values given in Ref. [15]. ^{c)} Values deduced from Ref. [17]. ^{d)} Value adjusted to give proton binding energy equal to the experimental separation energy. ^{e)} The spin orbit part of the captured proton potential is defined as

$$+a(l)\lambda_{\text{SO}} \left(\frac{\hbar}{2M_p c} \right)^2 V_0 (\exp x)(1+\exp x)^{-2}$$

where $\lambda_{\text{SO}} = 25$ and $a(l) = l$ for $j = l+1/2$ and $a(l) = -(l+1)$ for $j = l-1/2$.

with Julie. They are listed in Table III. In this analysis we have used the following normalization [11]:

$$\sigma(l, j) = 3.84 \frac{2J_f + 1}{2J_0 + 1} C^2 S(l, j) \sigma_{\text{Julie}}(l, j).$$

According to French *et al.* [12], for final states having the lowest isospin $T_f = T_0 - 1/2$, and for the transfer of a proton in the l, j shell model orbital, the sum rule is:

$$G(l, j) = \sum \frac{2J_f + 1}{2J_0 + 1} C^2 S(l, j) = \langle \text{proton holes} \rangle_j - \frac{1}{N - Z + 1} \langle \text{neutron holes} \rangle_j.$$

This rule predicts $G(3, 7/2) = 4$ and $G(1, 3/2) = 3.6$ respectively for the $1f_{7/2}$ and the $2p_{3/2}$ shell model orbital. Assuming that all the $l = 3$ and all the $l = 1$ observed transitions below 4 MeV correspond to transfers in respectively the $1f_{7/2}$ and $2p_{3/2}$ shell model orbital, the corresponding experimental values are 3.70 for the $1f_{7/2}$ orbit and 3.00 for the $2p_{3/2}$ orbit.

2.3. The $^{56}\text{Fe}(d, \alpha) ^{54}\text{Mn}$ reaction

The alpha particle spectrum obtained at $\theta_{\text{Lab}} = 30^\circ$ is shown in Fig. 5. The overall energy resolution is about 50 keV (F. W. H. M.). The energy calibration has been obtained from the known energies [1] of the alpha particles corresponding to the most intense transitions. The deduced excitation energies, the values of the cross-sections integrated between $\theta = 20^\circ$ and $\theta = 80^\circ$ and the values of the cross-sections at $\theta_{\text{Lab}} = 30^\circ$ are given in Table V (the level ordering is the same as in Table I and Table II). The values of the absolute cross-sections have been obtained by weighting the target we used. The systematic error about these values is about 30%.

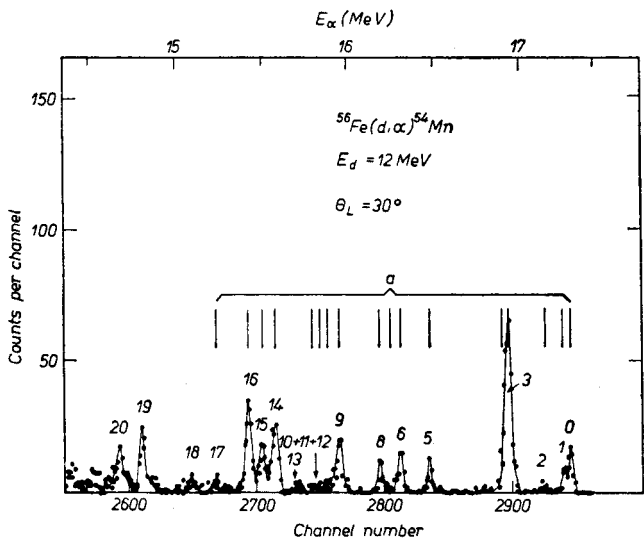


Fig. 5. Alpha particle spectrum from the $^{56}\text{Fe}(d,\alpha)^{54}\text{Mn}$ reaction. Previously known levels are labelled "a".

TABLE V

Experimental results of $^{56}\text{Fe}(d,\alpha)^{54}\text{Mn}$ reaction

Level N°	E_x (keV) a)	J^π b)	E_x (keV) c)	l c)	$\left.\frac{\partial\sigma}{\partial\Omega}\right _{30.8^\circ}$ $\mu\text{b/sr c}$	$2\pi \int_{20}^{90} \frac{\partial\sigma}{\partial\Omega} \sin\theta d\theta$ $(\mu\text{b c})$
0	0	3+	0		17.4 ± 2.2	114 ± 12
1	56 ± 12		51 ± 20		5.9 ± 1.3	29 ± 5
2	156 ± 12		151 ± 20			32
3	365 ± 12		366 ± 20		$92.9\pm 5.$	255 ± 12
4	405 ± 12					2
5	837 ± 12		835 ± 20		7.1 ± 1.3	26 ± 3
6	1008 ± 12		1008 ± 20		19.2 ± 2.6	100 ± 10
7	1074 ± 12					
8	1137 ± 12		1122 ± 20		7.5 ± 1.3	35 ± 5
9	1376 ± 12		1378 ± 20		25.6 ± 2.6	113 ± 11
10	1455 ± 12		1452 ± 20			46 ± 5
11	1511 ± 12					
12	(1543 ± 12)					
13			1629 ± 20			23 ± 5
14	1784 ± 12		1773 ± 20		27.8 ± 2.6	110 ± 11
15	1859 ± 12		1842 ± 20		14.2 ± 2.0	60 ± 10
16	1924 ± 12		1910 ± 20		44.5 ± 3.5	200 ± 20
17	2137 ± 12		2113 ± 20		4.81 ± 1.2	31 ± 7
18			2276 ± 20		6.64 ± 1.3	40 ± 7
19			2562 ± 20		27.6 ± 2.6	116 ± 12
20			2682 ± 20		13.2 ± 2	91 ± 13

a) Previously known values [1]. b) See Ref. [14]. c) This work.

As it has been shown in Ref. [6], the understanding of the (d, α) reactions induced on medium weight nuclei at $E(d) \simeq 12$ MeV, is not clear. So no analysis of the $^{56}\text{Fe}(d, \alpha)^{54}\text{Mn}$ data has been done, and the experimental results are presented here without comments.

2.4. Summary of the experimental data

In Fig. 6 we compare the values of the experimental integrated cross-sections of the transitions leading to the same final state in ^{54}Mn . For the $(^3\text{He}, p)$ spectrum, we give the L value of the transferred pair orbital momentum. For the $(^3\text{He}, d)$ spectrum, we give the l value of the transferred proton orbital momentum.

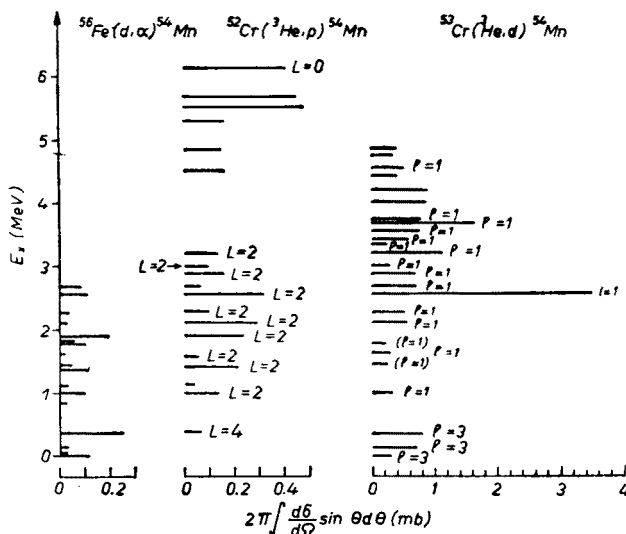


Fig. 6. Experimental integrated cross-section spectra for the $^{52}\text{Cr}(^3\text{He}, p)^{54}\text{Mn}$, $^{52}\text{Cr}(^3\text{He}, d)^{54}\text{Mn}$ and $^{56}\text{Fe}(d, \alpha)^{54}\text{Mn}$ reaction. The scale for the $^{52}\text{Cr}(^3\text{He}, d)^{54}\text{Mn}$ data is reduced by a factor five

It should be noted that the most intense transitions in the $(^3\text{He}, p)$ reaction correspond to $(^3\text{He}, d)$ transitions governed by $l = 1$. So the wave functions of these states in ^{54}Mn would contain components involving the $2p_{3/2}$ proton configuration.

3. Discussion

The values of the integrated cross-sections of the $(^3\text{He}, p)$ transitions to the low lying levels in ^{54}Mn have been computed with the wave functions proposed by Vervier [5]. We have also computed the cross-section of the $(^3\text{He}, p)$ transition to the analogue state, assuming that its wave function can be deduced in the same way as in Ref. [6] from that of the ^{54}Cr ground state (as deduced from the $^{54}\text{Cr}(^3\text{He}, \alpha)^{53}\text{Cr}$ results [13]). These results are compared to the experimental values in Fig. 7. We have normalized all the computed values so that the computed cross-section of the $(^3\text{He}, p)$ transition of the analogue state be equal to the experimental value. The normalization coefficient value is roughly the same as the value

obtained in the same way in the $^{54}\text{Fe}(^3\text{He}, p) ^{56}\text{Co}$ reaction analysis [6]. The agreement between the computed and the experimental values is quite poor: all the theoretical cross-sections are too large. The $(^3\text{He}, d)$ results, presented in section 2.2., show that the wave functions of the states lying upper $E_x = 1.0$ MeV contain components involving the $2p_{3/2}$ proton orbit. So the wave functions computed by Vervier for these levels are not correct be-

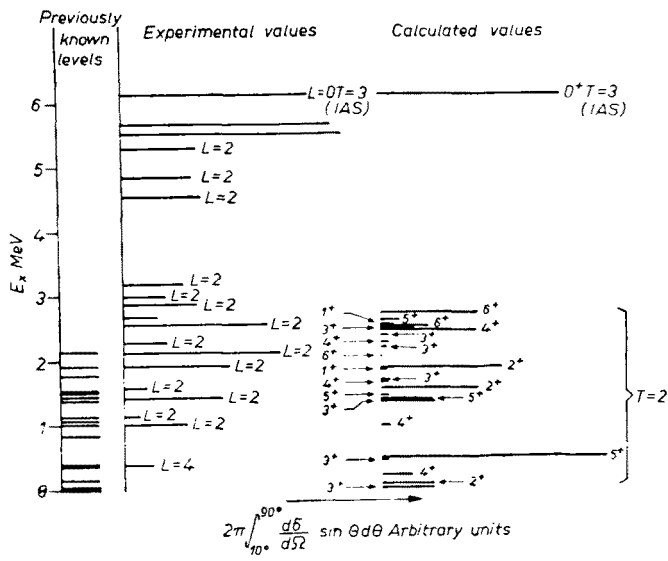


Fig. 7. Comparison between the experimental $(^3\text{He}, p)$ integrated cross-sections and the computed values

cause the configuration space he used is restricted to configurations in which protons remain in the $1f_{7/2}$ shell. It would be interesting to compute these wave functions in a greater configuration space.

In the framework of the pairing vibration model of Bohr [18, 19] a $J^\pi = 0^+ T = 2$ state at $E_x \simeq 1.5$ MeV is expected to be strongly excited in the $(^3\text{He}, p)$ reaction. On the other hand it has been suggested in Ref. [6] that a $J^\pi = 0^+, T = 2$ state mainly of the $[(\pi f_{7/2})^4_0 \pi p_{3/2}, \nu p_{3/2}]_{J^\pi=0^+}^{T=2}$ is expected at $E_x \simeq 2.24$ MeV.

No evidence for such a state is supported by our data. The only possible candidate is the level Nb 20 at $E_x = 2.690$ MeV, for which the corresponding proton angular distribution seems to show an $L = 0$ pattern, and which is reached in the $(^3\text{He}, d)$ reaction by an $l = 1$ transition. However our $(^3\text{He}, p)$ data, for this state, are so bad that the problem remains open. A restudy of the $^{52}\text{Cr}(^3\text{He}, p) ^{53}\text{Mn}$, with a better energy resolution, would be desirable.

We wish to thank Pr. O. Nathan for its interest to this work and Dr J. Vervier for sending us its unpublished ^{54}Mn wave functions. The solid state counters were made by Mrs Garin, and the targets by Miss Doury: they are gratefully acknowledged. One of us (J. K.) wish to thank Professor E. Cotton for the hospitality extended to him during his stage at C. E. N. Saclay.

Addendum. After this paper has been written, a similar experiment, performed by L. L. Lynn *et al.*, has been reported in, *Nuclear Physics* **A135**, 97 (1969). Their incident energies were not the same than ours (10.0 MeV for (^3He , d) and 11.0 MeV for (^3He , p)), and their results are somewhat different. The main difference is the observation of four $L = 0$ transitions, corresponding to low-lying states in ^{54}Mn . This discrepancy is partly explained by our poorer resolution (60 keV instead of 45 keV), in the case of two transitions, corresponding respectively to states in ^{54}Mn at 1.449 MeV and 2.497 MeV. The observed $L = 0$ transition leading to the 2.117 MeV level in ^{54}Mn is known to correspond to a doublet in ^{54}Mn , and the other component, which is not necessarily an $L = 0$ one, may have a different relative intensity at 18.0 MeV, so that the resulting angular distribution has no longer an $L = 0$ pattern. The same explanation may be valid for the $L = 0$ transition leading to the 1.917 MeV level in ^{54}Mn . This transition may be observed in our experiment by another one leading to the 1.857 MeV level in ^{54}Mn , and much weaker at an incident energy of 11.0 MeV than at an energy of 18.0 MeV. This assumption (the variation with incident energy of the intensities being not the same for different L -values) is supported by our observation of an $L = 2$ transition (numbered 18 in our paper) leading to the 2.268 MeV level in ^{54}Mn (a level which is populated in the (^3He , d) reaction), and which is not seen at all at 11.0 MeV.

REFERENCES

- [1] J. H. Bjerregaard *et al.*, *Nuclear Phys.*, **51**, 641 (1964).
- [2] B. Zeidmann *et al.*, *Phys. Rev.*, **120**, 1723 (1960).
- [3] J. L. Legg *et al.*, *Phys. Rev.*, **134**, B752 (1964).
- [4] L. Jonsson *et al.*, *Ark. Fys.*, **33**, 549 (1966).
- [5] J. Vervier, *Nuclear Phys.*, **78** 497 (1966); Private communication.
- [6] J. M. Laget *et al.*, *Nuclear Phys.*, **A125**, 481 (1969).
J. M. Laget, Thesis, CEA Report, CEA R-3572.
- [7] N. K. Glendenning, *Phys. Rev.*, **137**, B102 (1965); *Ann. Rev. Nuclear Sci.*, **13**, 191 (1963).
- [8] J. A. Cookson *et al.*, *Nuclear Phys.*, **A97**, 232 (1967).
- [9] J. H. E. Mattauch *et al.*, *Nuclear Phys.*, **67**, 1 (1965).
- [10] R. H. Bassel *et al.*, Report ORNL 3240.
- [11] R. H. Bassel, *Phys. Rev.*, **149**, 791 (1966).
- [12] J. B. French *et al.*, *Nuclear Phys.*, **26**, 168 (1961).
- [13] R. Bock *et al.*, *Phys. Letters*, **19**, 417 (1965).
- [14] Landolt-Börnstein, *Energy levels of nuclei, $A = 5$ to $A = 257$* , Springer-Verlag, Berlin 1961.
- [15] R. Bock *et al.*, *Nuclear Phys.*, **A92**, 539 (1967).
- [16] F. G. Perey, *Phys. Rev.*, **131**, 745 (1963).
- [17] C. R. Perey *et al.*, *Phys. Rev.*, **132**, 755 (1963).
- [18] A. Bohr, *Invited talk at the Dubna Conference*, July 1968.
- [19] O. Nathan, *Invited talk at the Dubna Conference*, July 1968.